Optical Design, Tolerance Analysis, and Baffling of Very High-Resolution Satellite Telescopes

Mohamed Metwally*, Taher M. Bazan*, Fawzy Eltohamy*, Mahmoud Fathy**

ABSTRACT

The telescope design of a very high-resolution earth observation satellite is a challenging task due to several constraints, including the size, mass, performance, tolerance and environmental aspects. However, the demand for very high-resolution satellite imagery has increased day by day due to the numerous commercial and military applications. In this paper, an optical configuration for a ground sampling distance (GSD) of 25 cm is investigated according to a definite mission statement. The configuration represents on-axis Korsch scheme with the advantage of small conic mirror constants without higher-order parameters. In addition, a tolerance analysis utilizing a Monte Carlo algorithm is performed. The suggested baffling arrangement based on a series of point sources with different off-axis angles is derived. The size of the telescope is applicable to be launched into space by the current launch vehicles.

KEY WORDS
Very high-resolution telescope, Korsch scheme, Baffling, Tolerance Analysis.

1. Introduction

The remote sensing is an interesting science and technology that give the ability to get a lot of information about the earth. The more information taken from images, the high-resolution telescopes are required. Therefore, improving the resolution of the remote-sensing satellite images is a critical issue. However, this target is considered as a challenge for the designers [1, 2].

With the huge technology revolution, many ideas take place to improve the design techniques of the earth observation telescopes. For example, the Korsch configuration is chosen as the best design concept for a compact optical telescope according to a comparative studies presented by Italian Space Agency [3] and Centre National d'Etudes Spatiales CNES [4]. On the other hand, off-axis three mirror anastigmatic (TMA) configuration provides a proper solution to satisfy the requirements of the high-resolution and wide swath [5]. If compared to Korsch schemes, TMA faces more challenges in design, measurements and alignment

---

* Egyptian Armed Forces
** Benha University

accuracy, according to the studies of Beijing Institute of Space Mechanics and Electricity (BISME) [5]. As a result, the Korsch scheme will be adopted in this paper as base line for the design of very high-resolution satellite telescope.

The mission statement in this paper is to utilize a telescope, with a panchromatic ground sampling distance (GSD) of 0.25 m and a swath width of 8 Km, within a satellite orbiting around the Earth in a sun-synchronous orbit with an inclination of 98.5° at 500 km altitude. The modulation transfer function (MTF) of the telescope should be not less than 0.25 including the optical manufacturing tolerance issue. The paper is organized as follows. The key design parameters of the telescope are investigated in Section 2. The design of the proposed optical scheme based on Korsch configuration is presented in Section 3. The tolerance analysis of the proposed system is investigated in Section 4 whereas the associated baffling design is derived in Section 5. Finally, Section 6 summarizes the conclusion.

2. Main Design Parameters

Starting from the mission statement, the main telescope parameters can be easily investigated as follows; the focal length f of the telescope in terms of satellite altitude H, detector pixel size Δ, and the GSD is given by [6]

$$f = \frac{H.\Delta}{GSD} \qquad (1)$$

Using a detector with pixel size of 10 μm [7] resulting in a focal length of 20m and this large focal length is expected since we are dealing with the very high-resolution task. According to the diffraction theory, the clear aperture D of the telescope is defined based on Rayleigh criterion as follow [8]

$$D = \frac{1.22\lambda f}{\Delta} \qquad (2)$$

where λ is the central wavelength of the panchromatic sensor. If the maximum wavelength is 0.4 μm and the minimum wavelength is 0.9 μm, then, the required clear aperture diameter will be 1400 mm and the telescope F-number is ~14.3. Although the value of D is quite high, many launchers have a wide fairing to accommodate such a telescope. For example, the Russian rocket Soyuz-2b with a payload fairing diameter of 3 m may be utilized as a launcher. To achieve the required swath width, the field of view of the telescope should be calculated as follows

$$FoV = 2tan^{-1}\frac{Swath}{2\,H} \qquad (3)$$

Thus, the FoV of 0.9167° is required to ensure a swath width of 8 Km at H = 550 Km. However, the design of the telescope should comply with these main parameters.

3. Korsch Telescope Design

A. Optical scheme

The proposed Korsch configuration is illustrated in Fig 1. The Korsch scheme consists of three on-axis aspheric mirrors (primary mirror M1, secondary mirror M2, and third mirror M3) with small conic constants. Two flat mirrors (M4 and M5) are employed as folding mirrors. The main characteristics of the utilized mirrors are

summarized in Table 1. Note that the conic constants of M1, M2, and M3 are applicable from the manufacturing point of view and the distance between M2 and M3 is ~ 3430 mm. In addition, the alignment of the proposed configuration is applicable because the three mirrors are on the same axis.

Table 1: Korsch Optical Design Parameters (units in mm)

Element	Radius	Thickness	Diameter	Conic	Y-shift
M1	4914.905	1961.331	1400	-0.97262	0
M2	-1301.961	3429.298	331	-2.36151	0
M3	1772.163	1069.599	270x120	-0.53112	-120
M4	Infinity	771.7647	145	0	0
M5	Infinity	888.274	160x50	0	90

B. Performance assessment

The next discussion is devoted to assessing the performance of the proposed Korsch telescope in terms of the major metrics such as MTF, spot diagram, field curvature and distortion. The performance of the Korsch scheme in terms of MTF is shown in Fig 2. It is obvious that MTF reaches 0.4 at a Nyquist frequency of 50 Lp/mm for the entire FoV even for sagittal or tangential directions.

Fig 3 shows the spot diagram of the proposed telescope for different angles within the required field of view. It is clear that the images at focal plane are confined to the pixel size of 10 μm. The associated field curvature and distortion are illustrated in Fig. 4. It is clear that the maximum field curvature is 0.047 mm and the maximum distortion is 0.368 %.

4. Tolerance Analysis

Generally, tolerance describes the visibility from the manufacturing point of view. The tolerance aspect can be described by the tolerance factor [4]. Taking the same reference tolerance budget presented in [4], the tolerance factor can be defined as the ratio between the resulted tolerance budget of the proposed design to the reference one. The more tolerance factor, the more manufacturing stability, i.e., the system can withstand more manufacture tolerance. Let T_X and T_Y are the tilting tolerance budget around X and Y-axes, respectively. Similarly, let D_X, D_Y and D_Z are the tolerance budget for displacement in the directions X, Y, and Z-axes, respectively. Consider ΔR is the tolerance in radius of curvature. Table 2 shows the tolerance budget for the proposed Korsch scheme based on the Monte Carlo algorithm with 1000 trials.

As a comparison, the proposed Korsch configuration gives a tolerance factor of 0.347 which is better than 0.27, the best tolerance factor achieved in reference [4]. Note that 90% of the trials achieve MTF greater than 0.348. Thus, the MTF including the tolerance issue satisfy the required MTF in the mission statement.

5. Korsch Baffling System

The baffling design is an important task to remove or minimize the stray light that may reach the photodetector. To achieve such a goal, the stray light power should be less than the detector noise power (dark current power) to get the best performance of the

Table 2: The Tolerance Budget

Objective Components	Tolerances type	Tolerances budget
Mirror 1 (Reference)	T_X & T_Y	1"
	Dx & D_Y	20
	ΔR	0.8 µm
Mirror 2	T_X & T_Y	5 "
	Dx & Dy	20 µm
	Dz	0.4 µm
	ΔR	1.4 µm
Mirror 3	T_X & T_Y	4 "
	Dx & D_Y	15 µm
	Dz	7.5 µm
	ΔR	6.5 µm
Mirror 4	Dz	87 µm
	ΔR	$R = 3 \times 10^7$ mm $\pm$ 0.015 µm
Mirror 5	Dz	45 µm
	ΔR	$R = 7 \times 10^6$ mm $\pm$ 0.714 µm
Focal block	Dx & D_Y	45 µm
	Dz	30 µm
Tolerance factor		0.347

optical system [9]. The received stray light power on the detector is usually described by the point source transmittance (PST) [10]. PST is defined as the irradiance at the reference plane (photodetector plane in our case) at a particular angle divided by the input irradiance for the same angle. The baffling design follows the same procedures presented in [10]. The starting point is to determine the critical elements; M1 opening hole, M3, M4, and M5. To minimize the number of these critical elements, blacked baffling plates (stops) will be used to reject the stray light as shown in Fig 5.

As shown in Fig 5, plate 1 blocks the stray light that may be reflected from M3 and reaches the focal plane whereas plate 2 blocks the stray light coming from M1 opening hole or M4. Therefore, the remaining critical element is M5. The next step is devoted to determine the illuminated objects. It is obvious that M1 opening hole is the key source of light of the Korsch system to enter the back box. To minimize the illuminated object seen by M5, M4 backside is already acting as a baffling plate; preventing the stray light to reach M5.

The next step is to determine all the rays pass from M1opening hole to incident on M5. As shown in Fig. 6a, there are three possible critical optical paths; paths no.1, 2,

4

and 3. In order to minimize the effect of these critical paths, three actions should be taken. Adding vans to M1 opening hole edges to minimize the effect of critical path no.1 and plates 3 & 4 for critical paths no. 2 and 3 as illustrated in Fig 6b. It is worth mentioning that the baffling design here assumes more than two reflections on the black surfaces will diminish the optical stray light power. Also, adjusting M3 dimension exactly with the FoV is necessary because increasing of M3 dimension will increase the possibility of stray light effect.

Now, the design of vans (numbers, heights and positions) is derived through the following procedure. Assume *r* be the radius of the main tube (containing M1, and M2), *a* be the M1 radius, and *S* be the length of the main tube. According to the variables illustrated in Fig. 7, x_n is the positions of the *n*th van while z_n is the position of the reflected ray after *n*th van. Starting with $x_0 = 0$, y_0 can be easily calculated according to the following relation

$$y_0 = a + S \tan^{-1}(FoV) \tag{4}$$

Then, x_1 and y_1 can be calculated by intersecting the line L_1 and FoV so that

$$x_1 = \frac{S(r_0 - y_0)}{2a + r_0 - y_0} \tag{5}$$

and

$$y_1 = \frac{a(r_0 - y_0) - r_0 y_0 + r_0^2}{2a + r_0 - y_0} \tag{6}$$

From figure trigonometry, the intersection of the line L_1 and the tube is given by

$$Z_1 = \frac{X_1(y_0 + r)}{r + y_0 - Y_1} \tag{7}$$

In general, the location of intersection between line L_n and the tube is expressed in terms of x_n and y_n as

$$Z_n = \frac{X_n(y_0 + r)}{r + y_0 - y_n} \tag{8}$$

By solving the line K_{n+1} and field of view, then

$$X_{n+1} = \frac{S^2(r - y_0) + S.Z_n(a + y_0)}{S(2.a + r - y_0) - Z_n(a + y_0)} \tag{9}$$

and

$$Y_{n+1} = \frac{S.r^2 - a^2.Z_n + S.a.r - a.r.Z_n + y0(a.Z_n - S.a - S.r + r.Z_n)}{2.S.a + S.r - S.y_0 - a.Z_n + y_0.Z_n} \tag{10}$$

By repeating the same sequence, the positions and heights of vans in the main tube are presented in Table 3 where the distance is measured from the primary mirror. Fig

Table 3: Vans heights and positions within the main tube (the unit in mm)

	1	2	3	4	5	6	7	8	9	10
Distance	51	181	308	433	556	676	793	908	1021	1131
Y-Radius	750	753	755	757	759	761	763	765	767	769
	11	12	13	14	15	16	17	18	19	20
Distance	1239	1345	1448	1550	1649	1746	1840	1933	2024	2113
Y-Radius	771	773	775	777	778	780	782	783	785	786

8 shows the position of the two groups of sharp edge vans with 90° tilting where the first group at the main tube and the second at the M1 opening hole.

Fig 8 shows the position of the two groups of sharp edge vans with 90° tilting where the first group at the main tube and the second at the M1 opening hole. Finally, the stray light power calculation for a series of off-axis cases of the point sources will be performed to check the overall baffling performance. Baffling simulation and evaluation are performed by Zemax [12].

Simulation Assumptions:
- The incident light on the telescope aperture is simulated as parallel rays with different inclination angles up to 80°.
- The telescope structure is coated with Chemglaze Z306 with silica powder as a black material since it gives a less than 7% Lambertian reflection in all directions [11].
- All mirrors are coated by Al with a reflection coefficient of 94 % [13].

However, based on the Landsat document [14], the typical value of the radiance reflected from the Earth is 40 W/m2µm sr within the spectral band of 4500 to 5150 nm and 23 W/m2µm.sr for the spectral band of 5000 to 6800nm, and these two bands cover the proposed telescope bands. Therefore, the irradiance incidents on the Korsch entrance pupil can be expressed according to the following relation

$$E_{ap} = \frac{L_E \times \Delta\lambda \times A_{ap}}{H} \qquad (11)$$

where L_E is the Earth irradiance and A_{ap} is aperture area. Thus, E_{ap} = 2.075×10⁻⁵ W/m². Also, the satellite bus which will carry the proposed telescope must satisfy the requirement that no shiny objects in the angle ±50° exist around the optical axis of the telescope. Additional external sun baffle is recommended to be used and fixed on the satellite panel. Nevertheless, the design of sun baffle is out of the scope of this study.

The simulation output covering all the incident angles is the distribution of PST as presented in Fig 9. According to the photodetector data sheet [7], it is clear that the design of the baffling system is affirmed since the stray light power is less than the detector sensitivity.

Finally, to show the advantages of the proposed telescope, a comparison between the design of the proposed telescope and that presented by CXCI program (related to

the French Space Agency) planned to be launched in 2020-2022 [4] is given in Table 4. It is clear that the proposed telescope is superior in most issues. However, to achieve more compactness to the proposed telescope, folding mirrors can be used without scarifying the performance but at the expense of the number of optical elements.

Table 4: A comparison between the proposed and CXCI optical designs

Parameter \ Type	Proposed telescope	CXCI design [4]
Resolution	0.25 m @ 500Km	0.3 m @ 700Km
F-number	F/14.3	F/20
MTF	0.348	0.34
Tolerance factor	0.347	0.27
X distortion	0.368%	0.9%
Y distortion	0.16%	0.3%
Number of optical elements	5	7
M1-M2 distance	1.961 m	1.8 m
Total axial telescope length	3.43 m	2.6 m

6. Conclusion

The optical design of a very high-resolution telescope with a GSD of 0.25m suitable for the next-generation earth observation system has been investigated. Several subjects are explored in details including the optical performance and tolerance analysis. Furthermore, the associated baffling system is derived and accurately simulated. The optical performance shows that the MTF of the proposed Korsch configuration is 0.35 with F-number of 14.3, and low field curvature and distortion values. The proposed telescope shows a powerful design in many aspects if compared to the recent studies.
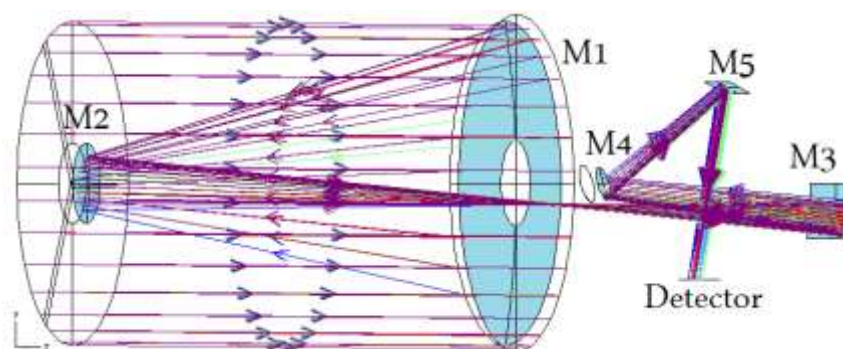
Figures

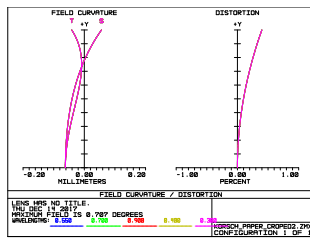

Fig 1 Layout of the proposed Korsch telescope

Fig 2 MTF curve for the proposed Korsch telescope

Fig 3 The spot diagram of the Korsch system

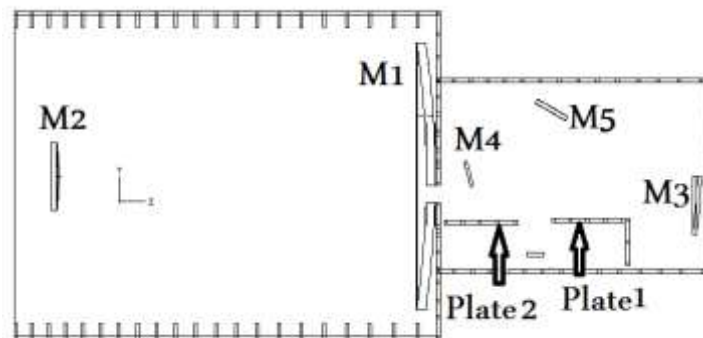Fig 4 Field curvature and distortion
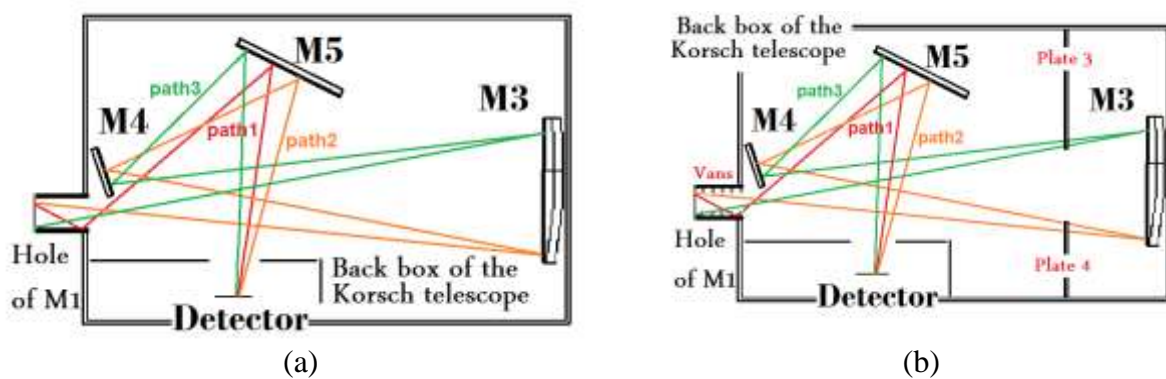

Fig 5 The position of plate 1 and 2

(a)

(b)

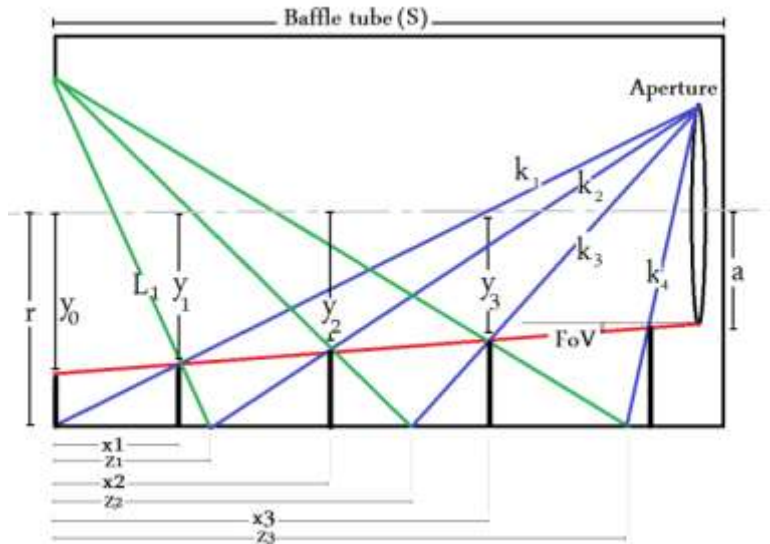Fig 6 The baffling design (a) Critical paths of the system (b) Critical paths removal through plates
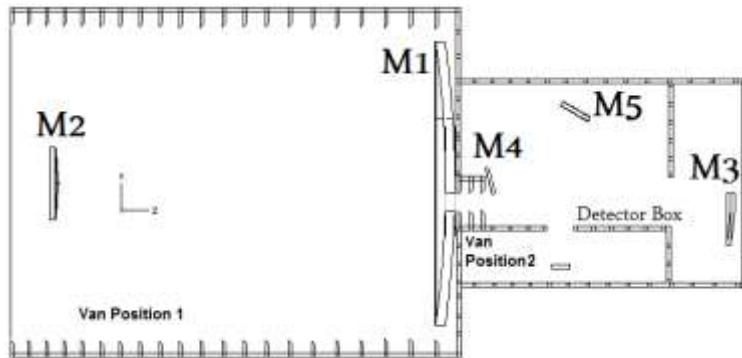
Fig 7 The vans parameters

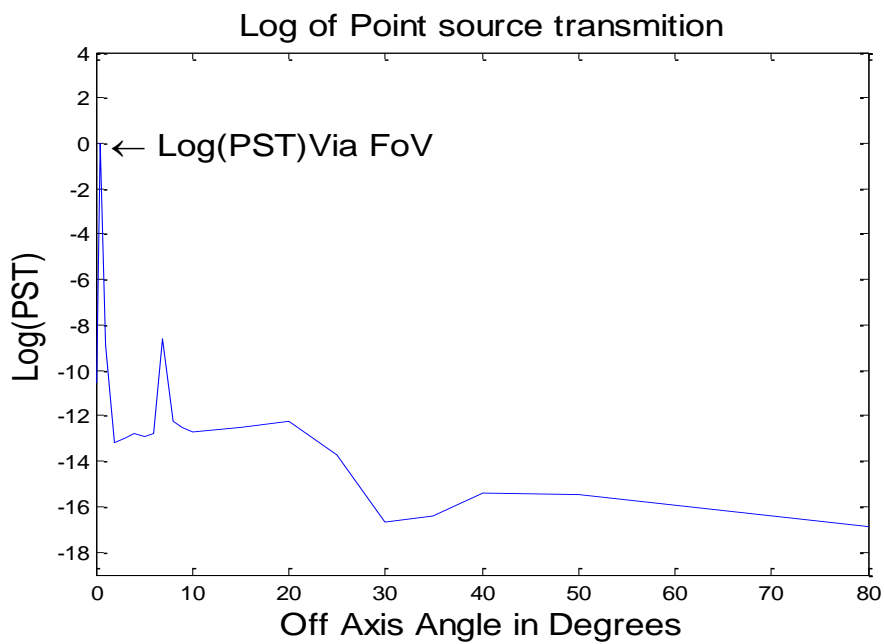Fig 8 Description of final baffling layout

Fig 9 The simulation output of the Korsch baffling system

References

[1] R. Woodruff, T. Hull, S. Heap, W. Danchi, S. Kendrick, and L. Purves, "Optical design for CETUS: a wide-field 1.5m aperture UV payload being studied for a NASA probe class mission study, "Proc. SPIE, Astronomical Optics: Design, Manufacture, and Test of Space and Ground Systems, 104011P, 2017.

[2] J.-M. Delvit, C. Thiebaut, C. Latry, G. Blanchet, "Wave front sensing for next generation earth observation telescope," International Conference on Space Optics (ICSO), France, 2016.

[3] F. Simonetti, A. Romoli, P. Mazzinghi, and V. Brantina, "Reflecting telescopes for an orbiting high-resolution camera for Earth observation," Opt. Eng. vol. 45, pp. 053001, 2006.

[4] V. Costes, G. Cassar, L. Escarrat, and S. Conseil "Optical design of a compact telescope for the next generation earth observation system" Proceedings of International Conference on Space Optical Systems and Application (ICSOS), 2012.

[5] B. FAN, W.-J. Cai, Y. Huang, "Design and test of a high performance off-axis TMA telescope" Proceedings of International Conference on Space Optical Systems and Application (ICSOS), 2012.

[6] N. Wanna, "Design of reflective optical systems," M.Sc. thesis, Faculty of North Carolina State University, pp. 26-27, 2006.

[7] ON Semiconductor "KLI-4104 Data sheet", www.onsemi.com, 2015 − Rev. 5.

[8] N. Menn, "Practical optics" Elsevier Inc, pp. 60-64, 2004.

[9] L. Scaduto, É. Carvalho, L. Santos, F. Yasuoka, M. Stefani, and J. Castro, "Baffle design and analysis of stray-light in multispectral camera of a Brazilian satellite", Annals of Optics, XXIX ENFMC, 2006.

[10] Robert P. Breault, "Control of Stray Light", in "Handbook of Optics", vol. 1, McGraw-Hill, New York, 1995, Chapter 38.

[11] R. Breault and S. Pompea, "Black surfaces for optical systems," in "Handbook of Optics", vol. 2, Second Edition, McGraw-Hill, New York, Chapter 37, 1995.

[12] A. Buffington, B. Jackson, and P. Hick "Calculations for, and laboratory measurements of a multistage labyrinthine baffle for SMEI," Proceedings of SPIE, vol. 4853, 2003.

[13] A. foster, T. Armstrong, P. Chadwick , and M. Held, "Dielectric coatings for IACT mirrors," International Cosmic Ray Conference, Rio De Janeiro, 2013.

[14] NASA internet site "Landsat 8 reference parameters" internet PDF document

[15] https://sustainablelandimaging.gsfc.nasa.gov/rfi/Landsat_8_Reference_Parameters.pdf.